

CHAPTER-6

Highly efficient reduced graphene oxide (rGO) Supported Acid-base bifunctional catalyst for Carbon-Carbon bond-forming Reactions Under solvent-free conditions

[6.1] Introduction

At present, acid-base bifunctional catalysis is of prime importance in organic chemistry in consequence of having low toxicity, operational simplicity, and superior accomplishment than individual acid and base catalysts, imparting a new benefaction in the advancement of green chemical processes [1]. For various chemical transformations in chemical industries and fine chemicals, a wide range of homogeneous acid-base catalysts have been employed so far [2, 3]. However, the conventional homogeneous catalysts are mainly endured from recyclability issues even though they are highly competent. On the contrary, heterogeneous catalysts have long been built up, which can be alienated from the products effortlessly [4]. Generally, solid acid catalysts are derived from metallic species like silica-alumina [5], silica-based mesoporous materials [6], mesoporous materials [7, 8], zeolites [9] and metal-organic frameworks (MOFs) [10, 11]. On the other hand, solid base catalysts such as alkaline earth oxides, alkali metals on supports, zeolites, AlPO, KNH_2 on alumina, KF on alumina, hydrotalcite, and oxynitrides have also been reported previously [12, 13, 14]. One of the problems associated with the aforesaid systems is their lifespan, owing to the strapping chemisorption of H_2O molecules on the active sites of the catalysts. To set the benchmark, water-forbearing solid catalysts with great recitation are needed [15]. In present-time, solid-supported bifunctional catalysts are of great significance facilitating well-organized organic transformations by exploiting two opposing functionalities without reciprocal devastation [16]. Graphene is becoming a “sparkling star” among all carbon allotropes [17]. The distinctive two-dimensional (2D) structures with remarkable properties such as hydrophobicity, stability, large specific surface area ($\sim 2630 \text{ m}^2 \text{ gm}^{-1}$), rich oxidative functionalities (such as $-\text{OH}$, $-\text{COOH}$, $-\text{C}-\text{O}-\text{C}$, and $-\text{C}=\text{O}$ groups), defect sites on the surface together with fascinating physical (electronic, mechanical, and thermal) properties [18,19,20] have been expected to resolve such aforesaid issues. Recently, Y. Wang et al. [21] have prepared graphene supported $\text{Ru}/\text{SO}_3\text{H}$ bifunctional catalyst for the catalytic conversion of levulinic acid (LA) in the aqueous phase. The strong acidity provided by SO_3H groups, which promotes the

dehydration of 4-hydroxyvaleric acid (HVA) to form gamma-valerolactone (GVL) at low temperature (50 °C) without sharply lessen the hydrogenation activity of Ruthenium (Ru). F. Zhang et al. [22] have fabricated acid-base bifunctional carbocatalyst by instituting organoamines on the basal planes of graphene oxide (GO), promoting one-pot Henry-Michael reactions with admirable activity to furnish multifunctional nitroalkanes. Through computational design, S. Liu et al. [23] have tested highly efficient bifunctional RuN₄ doped graphene (RuN₄-Gra) and modified RuN₄-Gra catalysts over both oxygen reduction and CO₂ reduction reactions. We have previously reported atypical highly proficient bifunctional FeNPs implanted on amino-modified reduced graphene oxide (FeNPs/Am@rGO) [where FeNPs = Fe nanoparticles; Am = Primary aromatic amine derivatives such as p-phenylenediamine (PPD) and/or aniline (AN)] catalysts for Knoevenagel condensation reaction [24].

In recent times, the progression of organic chemistry and avaricious its quintessence, one comes swiftly in our mind that carbon-carbon bond-forming reactions can play a major role in sculpturing this domain of science instead of any other organic reactions [25]. These reactions are one of the most pivotal and rudimentary reactions in organic chemistry to fabricate functionalized organic stuff with escalating intricacy, coherence and indistinguishability [26-28]. More particularly, carbon-carbon bond formation via Henry and Aldol condensation reactions are one of the noteworthy and most constructive reactions in the plentiful area such as pharmaceutical, cosmetic and agrochemical industries [29, 30]. W. Zhang and co-workers [29] have prepared a bifunctional GO–AEP–UDP catalyst using ureidopropyl (UDP) group as an acid and 3-[2-(2-aminoethylamino)ethylamino]-propyl (AEP) act as a base. This GO–AEP–UDP catalyst has shown superior catalytic performance in the classic Henry reaction of 4-nitrobenzaldehyde with nitromethane. E. Rodrigo et al. [30] have fabricated a heterogeneous bifunctional organocatalyst (rGO-NH) and used for archetypal organic transformations such as Knoevenagel, Michael and Aldol reactions. Based on the obtained results, a significant role is played by graphene support during these reactions. In this chapter, we report distinctive acid-base bifunctional

FeNPs implanted on amino-modified reduced graphene oxide [FeNPs/DETA@rGO, where, DETA= diethylenetriamine] catalyst and exemplify its astonishing catalytic activity over carbon-carbon bond-forming reactions especially for Henry and Aldol condensation reactions. We have evaluated various reaction parameters such as the impact of the amount of catalyst, mole ratio, various solvents, temperature and time to attain the optimized reaction conditions as well.

[6.2] Experimental section

(a) Materials

Nitromethane (CH_3NO_2) was procured from Spectrochem Pvt. Ltd. while, some other chemicals such as benzaldehyde, 4-methyl benzaldehyde, 4-methoxy benzaldehyde, 4-nitro benzaldehyde, 2-hydroxy benzaldehyde, furfuraldehyde, anhydrous FeCl_3 , and NaBH_4 were procured from S. D. Fine-Chem Ltd. Diethylenetriamine (DETA) was purchased from Chem-Dyes Pvt. Ltd. All of these reagents are of analytical grade and used as received without further purification.

(b) Synthesis of graphene oxide (GO) and reduced graphene oxide (rGO)

The graphene oxide (GO) was prepared according to the modified Hummers' method [31] and is already discussed in Chapter 2. Moreover, a chemical reduction method [32] has been preferred for the synthesis of reduced graphene oxide (rGO) and is given in Chapter 2.

(c) Synthesis of amine-functionalized graphene oxide (DETA@rGO)

DETA@rGO was prepared according to the method reported earlier [33]. In a general procedure, 500 mg of GO was dispersed in 100 mL deionized water and Sonicated for 10 min. After that, 1 g of diethylenetriamine (DETA) in 10 mL of deionized water was added drop-wise in the suspension of GO. The suspension mixture was allowed to stir for 12 h at room temperature. The resulting solid mixture was separated by centrifugation, washed with plenty of acetone and deionized water, and finally dried in a vacuum oven for 48 h.

(d) Synthesis of FeNPs/DETA@rGO bifunctional catalyst

As-synthesized 20 mg DETA@GO was dispersed in 10 mL of deionized water and was sonicated for 30 min at room temperature. Subsequently, 2 mmol of FeCl_3 dissolved in 5 mL of deionized water was added drop-wise into the suspension of DETA@GO which was being ultrasonicated for 20 min to produce a homogeneously dispersed suspension. After sonication, a freshly prepared NaBH_4 solution (5 mL) was slowly added into the suspension and the solution mixture was stirred continuously for 30 min at room temperature. The obtained product was isolated by centrifugation and washed with plenty of distilled water and finally dried in an air oven at 65 °C.

(e) Catalytic test

Henry Reaction

The Henry reaction was performed in a 50 mL three-necked round bottom flask equipped with a magnetic stirrer. In a general procedure: 20 mg of catalyst, a mixture of 5 mmol of benzaldehyde and 5 mmol of nitromethane as a nucleophile were added into the reaction vessel. The mixture was stirred at 50 °C for 2 h under nitrogen atmosphere. The organic aliquot was confirmed by a Chemito 8610 gas chromatograph (GC) equipped with DB-5 capillary column (30 m, 0.32 mm id, 0.25 mm film thickness). The catalyst was recovered after each run, washed with ethanol followed by distilled water, and later on dried in an air oven at 80 °C for 6 h before reuse.

Aldol Condensation reaction

The Aldol condensation reaction was carried out in a 50 mL three-necked round bottom flask equipped with a magnetic stirrer. The general procedure is as follows: 20 mg of catalyst, a mixture of 5 mmol of benzaldehyde and 5 mmol of acetone were added into the reaction vessel. The mixture was stirred at 50 °C for 2 h under nitrogen atmosphere. The organic aliquot was confirmed by a Chemito 8610 gas chromatograph (GC) equipped with DB-5 capillary column (30 m, 0.32 mm id, 0.25 mm film thickness). The catalyst was recovered after each run,

washed with ethanol followed by distilled water, and later on dried in an air oven at 80 °C for 6 h before reuse.

[6.3] Results and discussion

The as-prepared catalysts were substantiated by various physicochemical techniques such as FTIR, Raman, XRD, XPS, HR-TEM, and thermogravimetric analysis. The results are discussed in this section:

(a) FTIR spectral studies

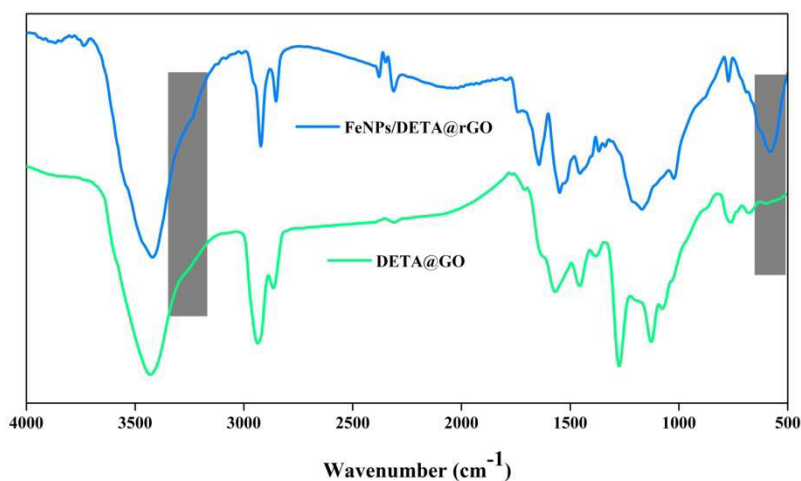


Figure 1 FTIR spectra of DETA@GO and FeNPs/DETA@rGO

The FTIR spectra of DETA@GO and FeNPs/DETA@rGO samples have shown in Fig. 1. In the FTIR spectra of both viz. DETA@GO and FeNPs/DETA@rGO, two bands observed in the region 3246–3181 cm^{-1} and 2863–2893 cm^{-1} , are assigned to $\nu(\text{N-H})$ and $\nu(\text{C-H})$ aromatic stretching vibrations, respectively, whereas, $\nu(\text{C=C})$ stretching vibration observed at $\sim 1598 \text{ cm}^{-1}$ [34]. One stretching vibration at 1307 cm^{-1} is attributed to C–N group in DETA@GO. After immobilization of FeNPs on the surface of graphene nanosheet, this band was shifted to lower frequency region at 1290 cm^{-1} in the spectra of FeNPs/DETA@rGO [35]. The $\nu(\text{C=O})$ band is observed in the region of 1720–1722 cm^{-1} (Chapter 2, Fig. 6) was disappeared in the spectra of DETA@GO, indicating the successful grafting of amino groups of diethylenetriamine derivatives on the surface of GO through the functionalization of $-\text{COOH}$ groups.

Besides this, one prominent peak at 1500 cm^{-1} is remained intact during *in situ* grafting of FeNPs as well as reduction of GO nanosheet, representing the flake-like nanosheet [35]. In the far-IR region, one supplementary band at 570 cm^{-1} in the spectra of FeNPs/DETA@rGO is assigned to $\nu(\text{M-O})$ stretching vibration band.

(b) Raman spectra

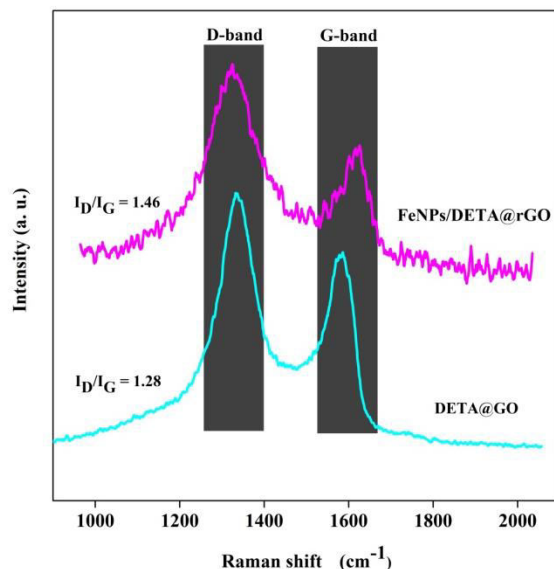


Figure 2 Raman spectra of DETA@GO and FeNPs/DETA@rGO

The Raman spectroscopy is one of the most constructive techniques for the enactment of lattice structure and morphological changes throughout the synthesis of catalysts [36-38]. The Raman spectra of DEPT@rGO and FeNPs/DETA@rGO samples have shown in Fig. 2. Two prominent peaks observed at ~ 1320 and $\sim 1556\text{ cm}^{-1}$ are attributed to the symmetry forbidden of the longitudinal plane phonon vibration or k-point phonons of A_{1g} symmetry (D-band) and the long-wavelength longitudinal phonon mode of graphene (E_{2g} phonon) (G-band) arises due to the sp^2 carbon network of the graphene plane, respectively [50]. Furthermore, the intensity ratio of D to G band (I_D/I_G) used to estimate the degree of disorder/order of a graphene-based material. The intensity ratio (I_D/I_G) for GO observed to be 0.99 (Chapter 2, Fig. 10), however, it was increased up to 1.28 and 1.46 for DETA@GO and FeNPs/DETA@rGO, respectively. This increasing

intensity ratio might be due to the incorporation of organoamine moieties and metal ions on the surface of the rGO nanosheet. In addition, we have checked the crystalline size of the synthesized catalysts by employing the Tuinstra–Koenig relation. With the aid of this equation, the inter defect distance calculated to be 13.09 and 11.47 nm for DETA@GO and FeNPs/DETA@rGO catalyst, respectively. [33]

(c) HRTEM study

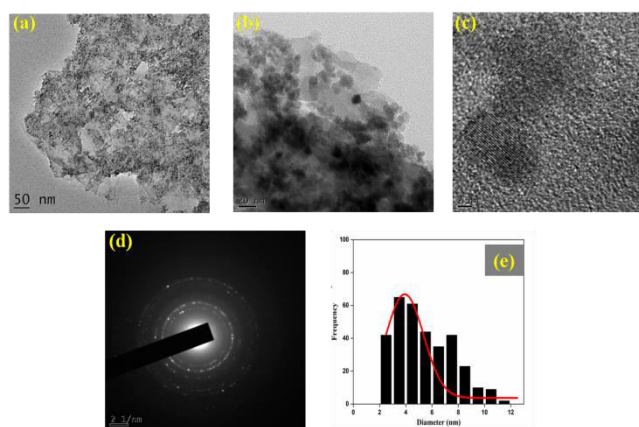


Figure 3 (a, b) Low magnification TEM image of FeNPs/DETA@rGO, (c) HRTEM image of FeNPs/DETA@rGO with fringe spacing, (d) SAED image of FeNPs/DETA@rGO, (e) Histogram graph of Fe nanoparticles

HRTEM images of FeNPs/DETA@rGO bifunctional catalyst have shown in Fig. 3. The TEM images [Fig. 3(a, b)] indicate that the Fe nanoparticles (FeNPs) had spherical shape and are uniformly dispersed on the surface of DETA@rGO nanosheet. The average size of FeNPs determined using ImageJ software and was found to be 3.9 ± 1.19 nm [Fig. 3(e)]. As can be seen in Fig. 3(c), the catalyst signifies the information about the crystal lattice fringes of FeNPs with a d -spacing of 0.21 nm, indicating with the plane of cubic FeNPs. The diffraction spot observed in the SAED image of FeNPs/DETA@rGO [Fig. 3(d)] revealed that the polycrystalline nature of FeNPs on the surface of the rGO nanosheet. These results are in well accordance with the XRD results as discussed below.

(d) TGA

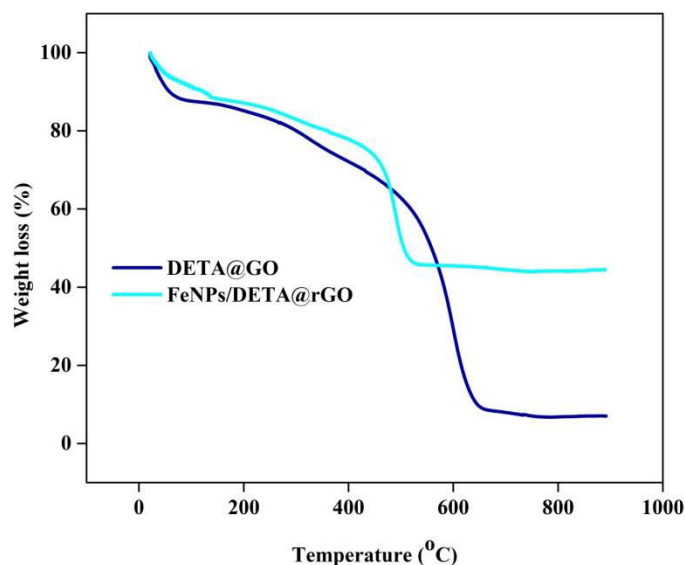


Figure 4 TG analysis of DETA@GO and FeNPs/DETA@rGO.

The quantitative assessment of the organic contents and the compositional stability of DETA@GO and FeNPs/DETA@rGO samples are acquired from the thermogravimetric (TG) analysis. TG analysis of as-prepared DETA@GO and FeNPs/DETA@rGO samples has performed and is shown in Fig. 4. The decomposition of the DETA@GO undergoes in three stages. First mass loss of 6.4% is observed in the temperature range 40–110 °C, supposed to be due to the liberation of trapped water molecules. The second (from 110–280°C) and third (from 280–650°C) stages may be due to the degradation of oxygen containing functional groups and the carbon skeleton. The observed mass losses in these temperature ranges are 9.6 and 72.8%, respectively. The thermal decomposition of bifunctional FeNPs/DETA@rGO catalyst undergoes in two stages (Fig. 4). The first stage which occurs in the temperature range 110–280°C with observed mass loss of 6.3% is corresponding to the decomposition of the oxygen containing functional groups. The second stage is related to the degradation of the carbon skeleton in the temperature range of 280–650°C, accompanied by a mass loss of 38.8%.

(e) XPS

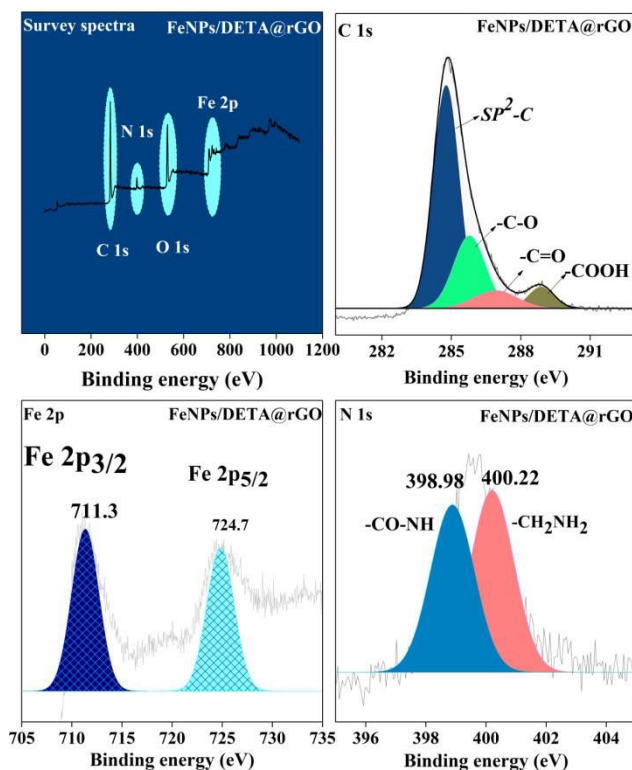


Figure 5 XPS spectra: (A) survey spectra, (B) C 1s spectra, (C) Fe 2p core level spectra, (D) N 1s spectra of FeNPs/DETA@rGO.

The surface chemical composition and bonding environment of bifunctional FeNPs/DETA@rGO catalyst is determined through XPS analysis. The XPS spectra are shown in Fig. 5. As can be seen in Fig. 5(A), the survey spectra of FeNPs/DETA@rGO demonstrate four well-known peaks at 281, 398.8, 530, and 720 eV, are assigned to C 1S, N 1S, O 1S and Fe 2p, respectively. While comparing C 1s spectra of GO (see Chapter 2, Fig. 9) with the high-resolution C 1s spectra of FeNPs/DETA@rGO [Fig. 5(B)] four prominent peaks observed at 286.4, 288.2, 289.3 and 291.3 eV, assigned to sp^2 -C, -C-O, -C=O, and -COOH, respectively. These results showed that the intensity of peaks for -C-O, -C=O and -COOH was considerably low and while the magnitude of sp^2 -C peak was significantly increased due to the re-establishment of the new in-plane sp^2 domains. The results are in good concurrence with the Raman results as discussed

above. Furthermore, the intensity peak of $-\text{COOH}$ group was much decreased as compared with C 1s spectra of GO due to the formation of amide groups by the reaction of DETA with carboxyl groups of GO. As depicted in Fig. 5(C), the Fe 2p core level spectra of exhibits two peaks at 713.5 and 725.3 eV, suggesting the presence of the Fe $2p_{3/2}$ and Fe $2p_{5/2}$, respectively. However, the high-resolution N 1s spectra of FeNPs/DETA@rGO [Fig. 5(D)] have shown two leading peaks with binding energies of 398.4 and 400.4 eV. They have been assigned to the formation of $-\text{CO}-\text{NH}$ and CH_2NH_2 , respectively. These results clearly confirm that the FeNPs are successfully attached on the surface of rGO nanosheet.

(f) X-ray diffraction patterns (XRD)

XRD is an imperative technique to examine the crystallinity of the as-prepared catalysts. The XRD patterns of DETA@GO and FeNPs/DETA@rGO samples are shown in Fig. 6. While comparing XRD patterns of GO sample (see Chapter 2, Fig. 8) with the DETA@GO sample, a basal reflection (002) peak at $2\theta = 11.8^\circ$ observed in GO sample is due to the intercalation of oxygen functionalities to the basal plane of GO [39]. On the contrary, the (002) reflection peak was slightly shifted to a lower angle ($2\theta = 10.6^\circ$) in DETA@GO sample compared to GO. This can be attributed to the grafting of diethylenetriamine on the surface of GO nanosheet [40]. Furthermore, a notable peak at $2\theta = 26.3^\circ$ observed in XRD pattern of GO, was slightly shifted to a lower angle ($2\theta = 23.6^\circ$) with broad intensity in DETA@GO sample. This was further substantiated that the stitching of the GO layers occurred during the preparation of DETA@GO sample by using diethylenetriamine as the alterer [40]. In addition to this, FeNPs/DETA@rGO sample shows peaks at $2\theta = 34.9, 43.4, 52.8, 56.3, 60.6,$ and 71.7 were assigned to (311), (400), (422), (511), (440), and (533) plane of crystallinity of Fe nanoparticles (JCPDS standard 19-0629 of Fe), respectively. From the XRD results, we can say that the successful immobilization of FeNPs on the surface of GO nanosheet was further corroborated by the surface area electron diffraction (SAED) pattern in the HRTEM analysis.

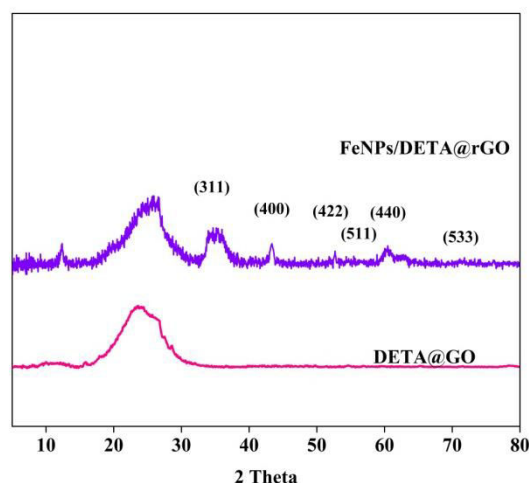
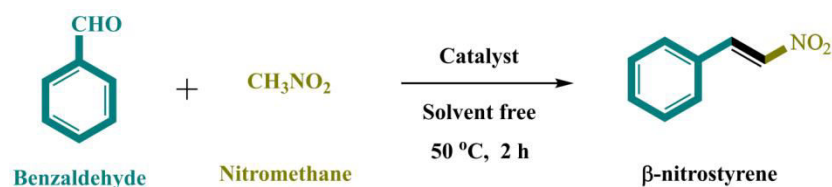


Figure 6 XRD patterns of DETA@GO and FeNPs/DETA@rGO.

[6.4] Catalytic Activity

(a) Henry reaction

The *Henry reaction* is a typical paradigm of carbon-carbon bond *formation* reaction in organic chemistry giving an absolute selective product i.e. β -nitrostyrene (Scheme 1).



Scheme 1 A schematic representation of Henry reaction.

We have studied the Henry reaction between benzaldehyde and nitromethane to give the selective nitroaldol addition product in the presence of various catalysts such as graphite flakes, GO, DETA, DETA@GO, FeNPs/DETA@rGO (Fig. 7). Blank experiments were performed over graphite flakes and GO show a lesser amount of percentage conversion and selectivity. Interestingly, GO-supported such as base functionalized i.e. DETA@GO and acid-base bi-functionalized i.e. FeNPs/DETA@rGO catalysts gave 82.6% and 89.5% conversion with the absolute β -nitrostyrene product selectivity of 89.5%

and 95.5%, respectively, indicating that both Lewis acidic (FeNPs) and basic sites (DETA) on the GO support were the real active precursors. In general, the Henry reaction would involve the addition of nitronate ion to a carbonyl compound [41]. One of the most basic sites created via attachment of an aldehyde substrate (aldimine intermediate) to the supported catalyst (Scheme 2) can facilitate this reaction, generating a nitroate ion via in situ deprotonations of a nitroalkane. However, FeNPs as Lewis acidic sites or both acidic and basic sites onto FeNPs/DETA@rGO bifunctional catalyst can facilitate the nitroaldol addition reaction; the former one activates the carbonyl group of an aldehyde substrate and the latter exerts as a combination of Lewis acid-Brønsted base that triggers and brings both reactants together [42], giving the nitroaldol addition product. To explore the support effects related to GO, we tested the catalytic activity of pure diethylenetriamine (DETA) and pure Fe metal salt solution as homogeneous catalysts, which gave significantly lower conversions viz. 42.6% and 10% with 45.9% and 25.3% of β -nitrostyrene selectivity. Therefore, FeNPs/DETA@rGO bifunctional catalyst has found to be a suitable candidate and preferred as a representative catalyst for further studies.

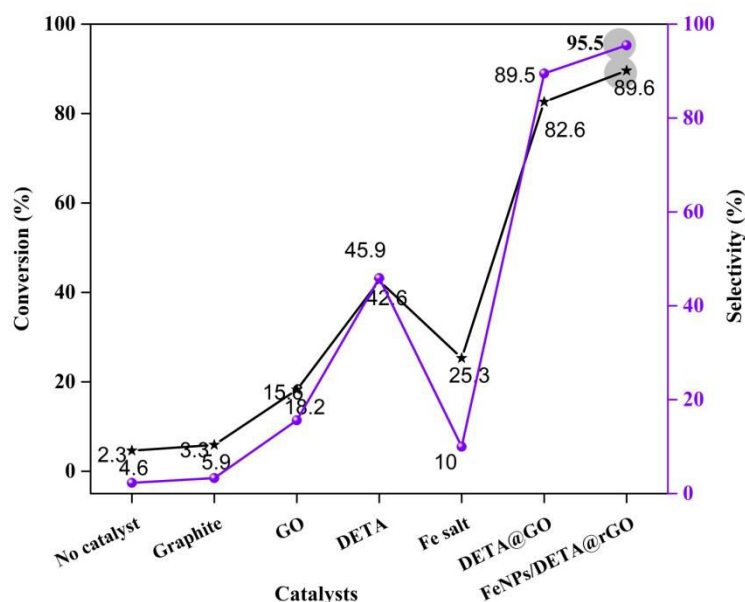


Figure 7 The catalytic activity of various catalysts for Henry reaction.

Reaction conditions: benzaldehyde (5 mmol), Nitromethane (5 mmol), varying catalysts (20 mg), Toluene (5 mL), temp. (50 °C), Time (2 h)

a) Effect of catalyst dosage:

The catalyst concentration is one of the decisive factors in the Henry reaction. We investigated the effects of amount of catalyst on the aforementioned reaction by keeping other parameters fixed. As shown in Fig. 8, four various dosages viz. 10, 20, 30, and 40 mg of FeNPs/DETA@rGO as a representative catalyst were used. Among them, the upmost of 89.6% benzaldehyde conversion with 95.5% selectivity of β -nitrostyrene product was monitored with 20 mg of catalyst dosage. Further upsurges in catalyst dosage observe no noteworthy difference in conversion but the selectivity of β -nitrostyrene was dwindled (Fig. 8), perhaps due to the formation of by-products. Therefore, the optimum dosage of the catalyst is considered to be 20 mg for the further study.

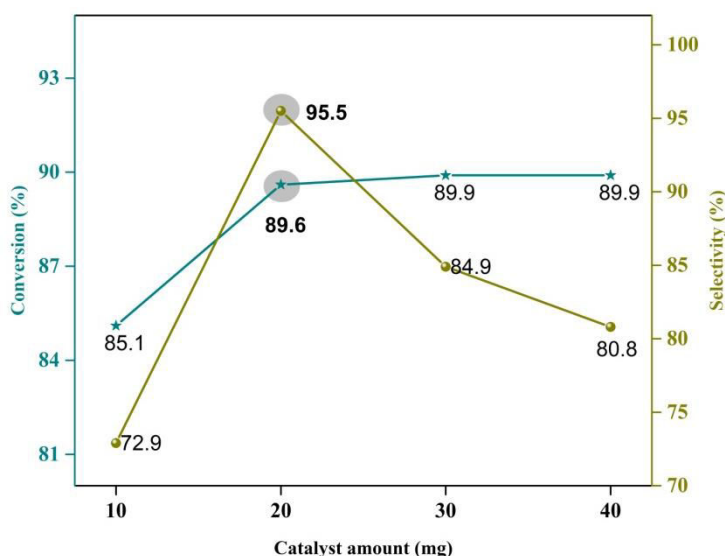


Figure 8 The influence of catalyst dosage for Henry reaction.

Reaction conditions: benzaldehyde (5 mmol), nitromethane (5 mmol), FeNPs/DETA@rGO (X mg), Toluene (5 mL), temp. (50 °C), time (2 h)

b) Effect of solvent

The effect of distinct solvents such as polar protic (water), polar aprotic (dichloromethane, DCM), and non-polar (toluene) was studied for this Henry nitroaldol addition reaction by keeping other parameters fixed. As shown in Fig. 9, conversion of benzaldehyde and β -nitrostyrene product selectivity was observed to be declining in the order of: toluene (89.6 %, 92.5%) > water (75.6%, 70.6%) > dichloromethane (72.3%, 69.7%). Among them, toluene with unmatched dilution factor provides enhanced conversion and selectivity. However, a simple, mild-mannered and proficient procedure for Henry reaction is in high demand for eternity in the domain of organic synthesis. With such inspiring protocol, we make use of efficacious and more environmentally benign route by employing the aforesaid reaction under solvent-free condition. The exemplary results of benzaldehyde conversion (92.3%) and selectivity of β -nitrostyrene (95.8%) were observed under solvent-free condition. That's why; we preferred solvent-free condition for the further experiments.

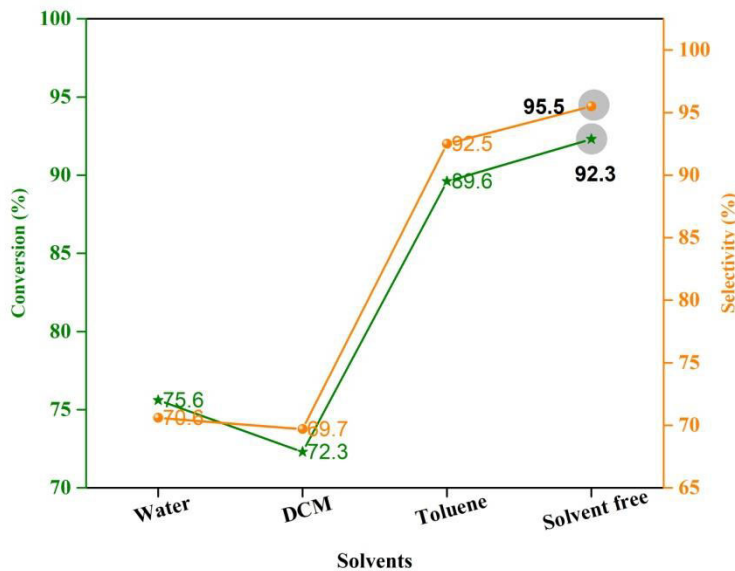


Figure 9 The influence of various solvents for Henry reaction.

Reaction conditions: benzaldehyde (5 mmol), nitromethane (5 mmol), FeNPs/DETA@rGO (20 mg), **various solvents** (5 mL) and solvent-free condition, temp. (50 °C), time (2 h)

c) Effect of Temperature

The catalytic conversion and selectivity of the product for the Henry reaction were persuaded by distinct temperature (Fig. 10). As noticed, the prevailing trend of escalating reaction temperature also uplifts substrate conversion, although, during a change of temperature from room temperature (RT) to 50, 70, 90 and 110 °C, the believed trend was monitored. In contrast, the reciprocal trend was observed in β -nitrostyrene product formation. Maximum selectivity of 95.5% was achieved at 50 °C however; the selectivity demonstrated a radical reduction of 90.5% while increasing the temperature to 70 °C. On a further rise in temperature to 90 and 110 °C, the trend continued to decrease with 80.9% and 75.5% product selectivity, respectively. This diminution was perhaps attributable to the formation of by-product i.e. nitro alcohol. Looking at the aim of the selective product i.e. with 95.5% was achieved at 50 °C and increase in temperature showed dramatically decrease in the yield of the product. As a result, the reaction temperature was fixed at 50 °C for further optimization.

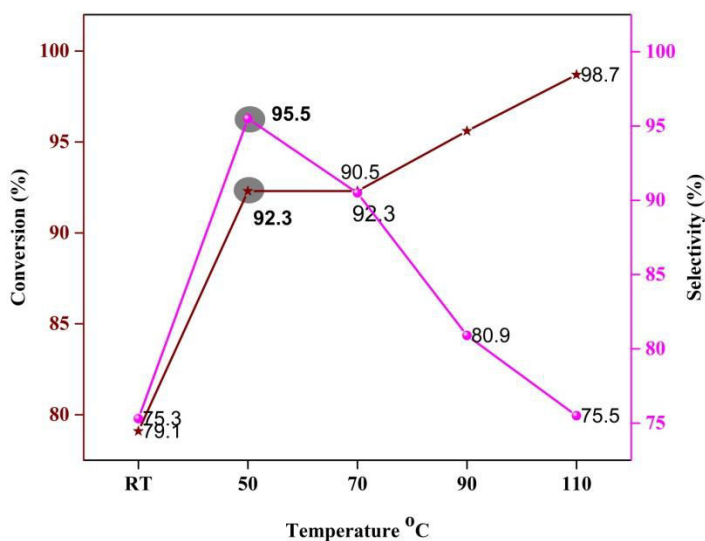


Figure 10 The influence of varying temperature for Henry reaction.

Reaction conditions: benzaldehyde (5 mmol), nitromethane (5 mmol), FeNPs/DETA@rGO (20 mg), solvent-free, **temp.** (X °C), time (2 h)

d) Effect of Time

The influence of reaction time is a momentous factor in the Henry reaction that permits us to determine the optimal time for accomplishing desired conversion and product selectivity. As shown in Fig. 11, we have checked the aforesaid reaction using varying time intervals viz. 30 min, 1, 2, 3 and 4 h. It was noticed that both % conversion and selectivity increased with foregoing reaction time and achieved maximum product selectivity i.e. 95.5 % in 3 h. However, the reaction time was lengthened for 4 h; there was no change in the conversion and product selectivity. For that reason, we have preferred maximum time 3 h for this reaction to ensure further parameters.

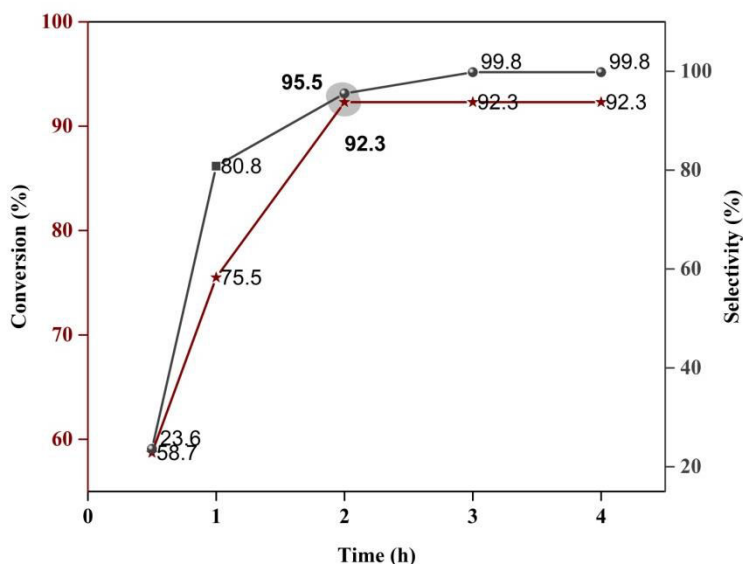
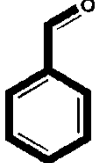
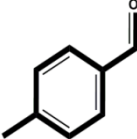
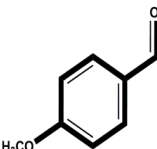
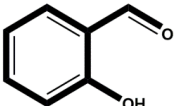
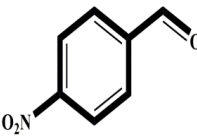
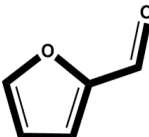


Figure 11 The influence of varying time intervals for Henry reaction.

Reaction conditions: benzaldehyde (5 mmol), nitromethane (5 mmol), FeNPs/DETA@rGO (20 mg), solvent-free, temp. (50 °C), **time (X h)**.

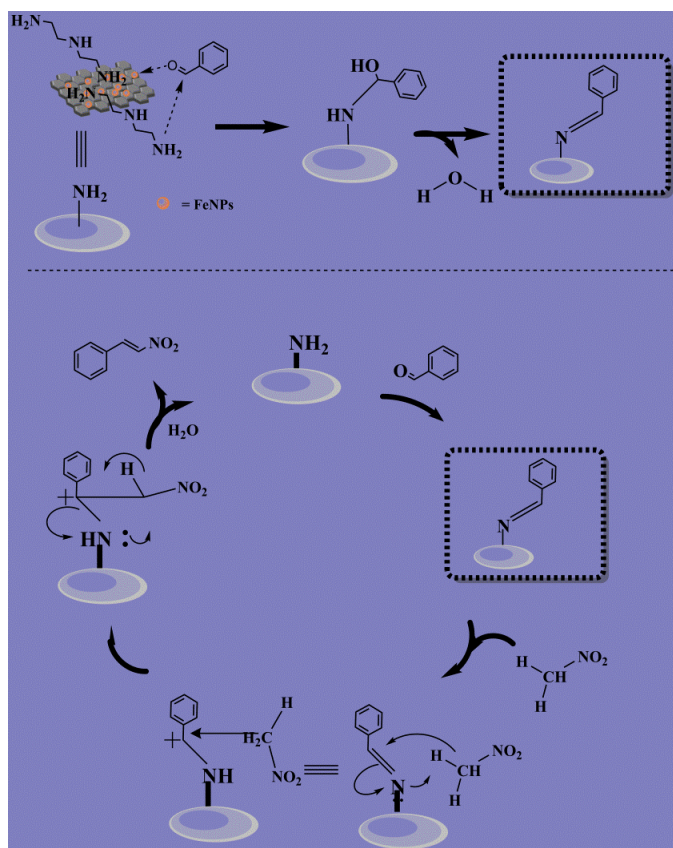
[6.5] Henry reaction using diverse aldehydes over FeNPs/DETA@rGO as a representative catalyst (Table 1)

$ \begin{array}{c} \text{R}-\text{CHO} + \text{CH}_3\text{NO}_2 \xrightarrow[50\text{ }^\circ\text{C}]{\text{FeNPs/DETA@rGO, 3 h}} \text{R}-\text{CH}=\text{CH}-\text{NO}_2 \\ \text{(A)} \qquad \qquad \text{(B)} \qquad \qquad \qquad \qquad \qquad \qquad \qquad \qquad \text{(C)} \end{array} $			
Entry	Substrat (A)	Conversion (%)	Selectivity (%)
1		92.3	99.8
2		68.1	83.8
3		66.6	72.6
4		49.8	39.6
5		47.6	38.5
6		71.2	73.5

Reaction conditions: Varying aldehydes (5 mmol), nitromethane (5 mmol), FeNPs/DETA@rGO (20 mg), solvent-free, temp. (50 °C), time (3 h).

After being successfully completed the optimized reaction conditions for the Henry reaction, probability and constrains of FeNPs/DETA@rGO catalyst were extended and examined between assorted aldehyde derivatives and nitromethane. As shown in Table 1, nitromethane reacted fruitfully with varying benzaldehyde derivatives (such as 4-methyl benzaldehyde, 4-methoxy benzaldehyde, 2-hydroxy benzaldehyde, 4-nitro benzaldehyde and furfuraldehyde) to give corresponding nitroaldol addition products. Taking FeNPs/DETA@rGO as a representative catalyst under solvent-free condition, the reaction was completed within 3 h (Table 1). Moreover, various aromatic aldehydes including electron-withdrawing (like 4-methyl benzaldehyde, 4-methoxy benzaldehyde and 2-hydroxy benzaldehyde), electron donating (4-nitro benzaldehyde) and hetero atom (furfuraldehyde) groups effectively coupled with nitromethane to furnish β -nitrostyrene selective product with excellent conversion and selectivity (Table 1, entry 2-6). Looking to the observed results (Table 1), the electron withdrawing groups have shown admirable conversion and selectivity except for 2-hydroxy benzaldehyde which has afforded slightly inferior reactivity might be due to the steric impediment factor [43]. Besides, electron donating group i.e. 4-nitrobenzaldehyde with nitromethane demonstrated analogous trend as of 2-hydroxy benzaldehyde [43]. Additionally, we have checked heteroatom compound i.e. furfuraldehyde with nitromethane, transforming to the desired product with almost good conversion and product selectivity (Table 1).

[6.6] The plausible reaction mechanism for Henry reaction using FeNPs/DETA@rGO as a representative catalyst



Scheme 2 The plausible reaction mechanism for the Henry reaction using the FeNPs/DETA@rGO catalyst

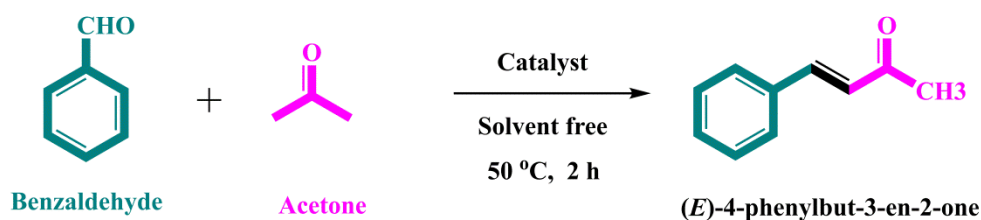
The probable reaction mechanism for the Henry reaction using FeNPs/DETA@rGO as a representative catalyst (where FeNPs act as Lewis acidic sites and NH_2 groups of DETA provide basic sites) is being shown in Scheme 2. Generally, the Henry reaction occurs through addition of nitronate ion to a carbonyl compound [41]. As shown in Scheme 2, the first step would involve the attachment of an aldehyde substrate to the FeNPs/DETA@rGO catalyst, engendering an aldimine intermediate with having most basic nature. In the next consecutive step, the aldimine intermediate with most basic sites can generate a

nitroate ion via in situ deprotonations of a nitroalkane. Besides this, FeNPs which provides Lewis acidic sites or FeNPs/DETA@rGO as a bifunctional catalyst can facilitate the nitroaldol addition reaction. In the same, former one activates the carbonyl group of an aldehyde substrate and the latter exerts as a combination of Lewis acid-Brønsted base triggers and brings both reactants together [42], giving the desired nitroaldol addition product.

[6.7] Catalytic activity of Aldol condensation reaction

(b) Aldol condensation reaction

Since, bifunctional FeNPs/DETA@rGO catalyst is expected to have broad prospects in carbon-carbon coupling reactions and has shown attention-grabbing results over Henry reaction as portrayed above. By keeping this view in our mind, we have decided to extend our study by ensuring its catalytic aptitude over Aldol condensation reaction (Scheme 3)



Scheme 3 A schematic representation of Aldol condensation reaction.

To weigh up the best-suited catalyst, we have tested various catalytic systems such as pristine graphite flakes, GO, pure DETA, Fe metal salts, DETA@GO, FeNPs/DETA@rGO over the Aldol condensation reaction using benzaldehyde and acetone as starting reagents with toluene as a non-polar solvent to form benzylideneacetone (one of flavouring ingredient in food and perfumes) as the principal product. The results are depicted in Fig. 12. It was indubitably contemplated from the figure that pristine graphite flakes, GO and without a catalyst have shown diminutive conversions while pure DETA exhibited fairly ameliorated conversion of benzaldehyde. On the other hand, pure Fe metal salt

showed comparable conversion with that of pristine graphite flakes, GO and without a catalyst. Through DETA@GO and FeNPs/DETA@rGO catalysts, higher catalytic conversions of benzaldehyde (i.e. 71.5 % and 81.2 %) were observed with 69.1 % and 74.2% selectivity of benzylideneacetone product, respectively. The aforesaid results which underpin the vital role of both FeNPs as Lewis acid and NH_2 group of DETA as basic sites steer the formation of aldimine intermediate by activating carbonyl group of aldehyde and the attachment on the supported catalyst [44]. In addition, the further reaction occurs through the formation of carboanion ($\text{CH}_3\text{COCH}_2^-$) via deprotonation of acetone molecule activated by aldimine intermediate, which is normally stronger than amine and more reactive than primary aldehyde [45]. It was succeeded by the addition-elimination reactions bringing about the formation of the desired product. Therefore, FeNPs/DETA@rGO has chosen as a representative catalyst for further experiments.

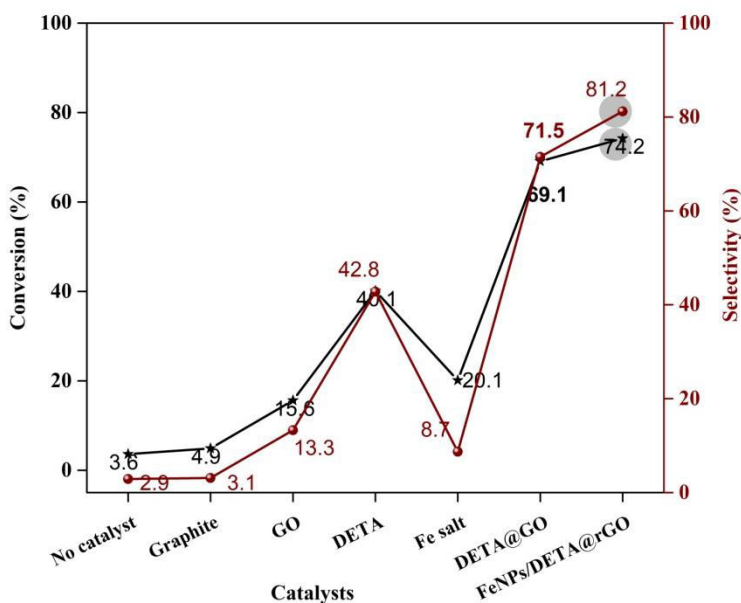


Figure 12 The catalytic activity of various catalysts for Aldol condensation reaction.

Reaction conditions: benzaldehyde (5 mmol), acetone (5 mmol), varying catalysts (20 mg), Toluene (5 mL), temp. (50 °C), time (2 h)

a) Effect of catalyst dosage:

As shown in Fig. 13, we noticed that the catalyst concentration was necessary in catalytic reaction and here, various catalyst concentrations such as 10, 20, 30, 40 mg are taken for the aforesaid reaction. As shown in Fig. 13, among the various catalyst concentrations, 30 mg is preferred for the aforesaid catalytic reaction achieving superlative benzaldehyde conversion of 74.2% with 81.2% of benzylideneacetone product selectivity. A further rise in the catalyst amount from 30 mg to 40 mg; observes minor increase in conversion from 74.2% to 74.6% however, selectivity was dropped down to 76.6%. This reduction is believed to be due to the dimerization of the olefinic molecule and/or further condensation of the product. Consequently, 30 mg of catalyst concentration was chosen for further optimized conditions.

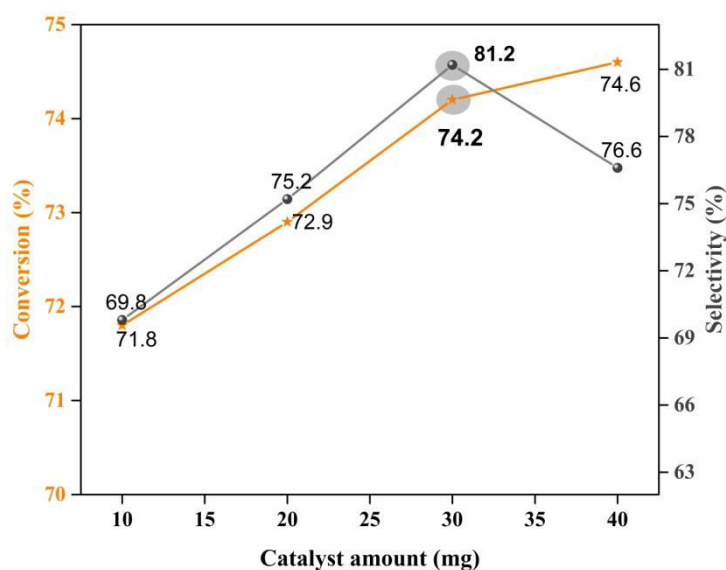


Figure 13 The influence of catalyst dosage for Aldol condensation reaction.

Reaction conditions: benzaldehyde (5 mmol), acetone (5 mmol), FeNPs/DETA@rGO (X mg), Toluene (5 mL), temp. (50 °C), time (2 h).

b) Effect of solvent

After successive experiment achieving the desired product through the investigation of catalyst concentrations, in the next succeeding step has to check another crucial parameter i.e. impact of solvent. Hence, we decided to examine the effect of various solvents such as polar protic i.e. water, polar aprotic i.e. dichloromethane (DCM) and non-polar i.e. toluene for the Aldol condensation reaction. Here, toluene has given unmatched dilution aspect providing better benzaldehyde conversion of 74.2% and 81.2% of benzylideneacetone product selectivity. However, our motive behind the study was to improve the desired product by decreasing the side-product using a non-hazardous solvent. Therefore, to achieve a simple, mild and efficient procedure for Aldol condensation reaction we have utilized effectual and greener route by employing this reaction under solvent-free condition. The splendid results of benzaldehyde conversion (88.6%) and selectivity of benzylideneacetone (82.9%) were achieved under solvent-free condition. In reply to the results obtained; we utilized solvent-free condition for further experiments.

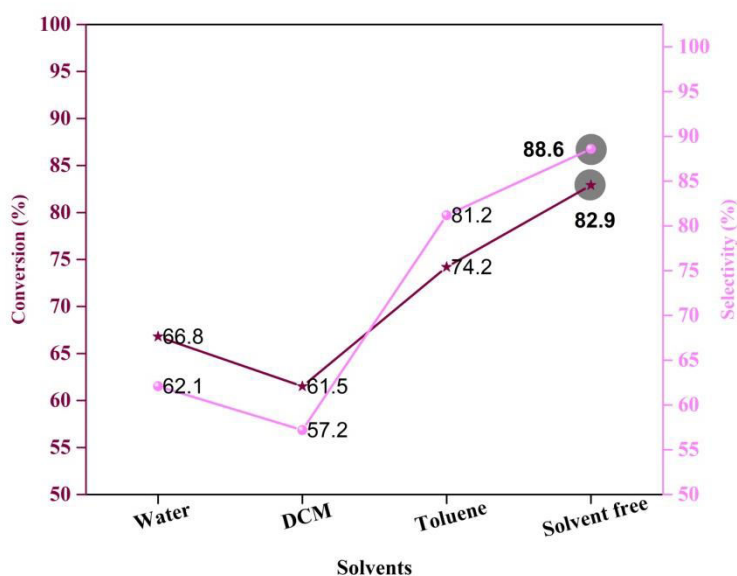


Figure 14 The influence of various solvents for Aldol condensation reaction.

Reaction conditions: benzaldehyde (5 mmol), acetone (5 mmol), FeNPs/DETA@rGO (30 mg), **various solvents** (5 mL) and solvent-free condition, temp. (50 °C), time (2 h).

c) Effect of Temperature

The effects of five different reaction temperatures such as room temperature (RT), 50, 70, 90 and 110 °C on the Aldol condensation reaction are illustrated in Fig. 15. It is discernible from the figure that 69.1% of benzaldehyde conversion with 70.2% of product selectivity was achieved at the ambient temperature. On rising the temperature to 50 °C, 82.9% of benzaldehyde conversion with utmost 88.6% of benzylideneacetone product selectivity was achieved. The progression of further rise in the temperature to 70 °C, an infinitesimal lift in the conversion of benzaldehyde was observed, however, the selectivity was dropped-down to 86.1%. It was decided to further incrementing in the temperature from 70 °C to 90 °C and then extended up to 110 °C, however, the similar trend was observed (Fig. 15). The possible reason for this reduction in the selectivity might be due to the dimerization of the olefinic molecule or further condensation of the product. Subsequently, 50 °C is chosen as a representative temperature for further studies.

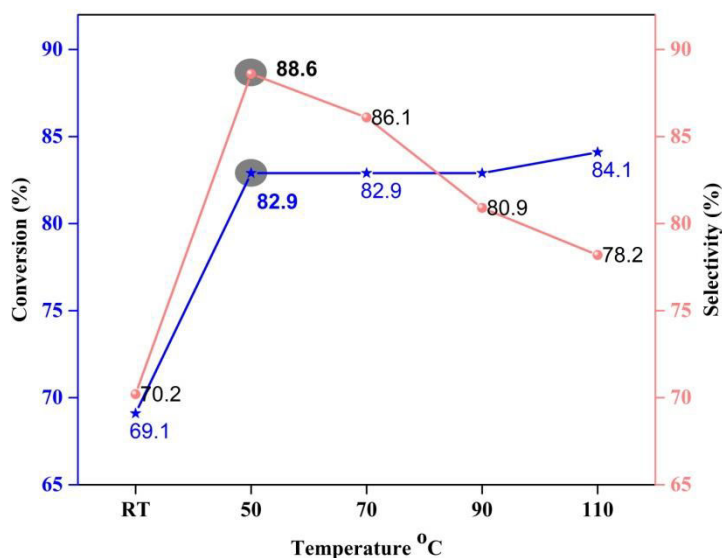


Figure 15 The influence of temperature for Aldol condensation reaction.

Reaction conditions: benzaldehyde (5 mmol), acetone (5 mmol), FeNPs/DETA@rGO (30 mg), solvent-free condition, **temp.** (X °C), time (2 h).

d) Effect of Time

For a typical Aldol condensation reaction, it is rather decisive to finish the reaction at the precise time to succeed in accomplishing higher conversion of benzaldehyde and the product selectivity. By keeping such intend in our mind, we have performed this reaction at varying time intervals, viz. 30 min, 1, 2, 3 and 4 h (Fig. 16). 51.3% conversion of benzaldehyde is achieved in the first 30 min but the selectivity for benzylideneacetone is found to be 31.6%. On further continuing the reaction to 1 h 72.1% and 69.8% of conversion and selectivity are observed, respectively. After the examination of the reaction mixture drawn at 4 h, it was noticed that conversion increased up to 82.9% with 96.7% selectivity of benzylideneacetone. However, on further continuing the reaction for 6 h, no change in the conversion (82.9%) and selectivity (96.7%) is observed. Therefore, we have chosen the reaction time as 4 h to achieve other parameters.

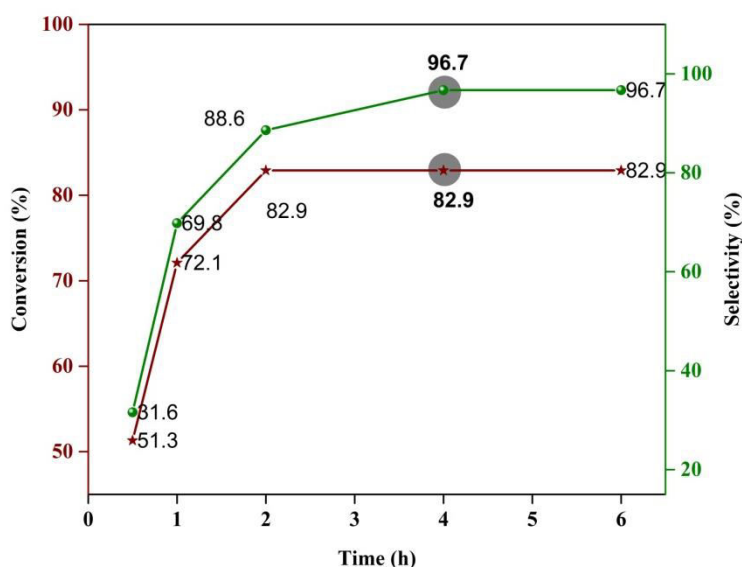
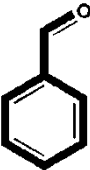
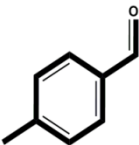
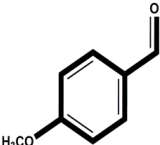
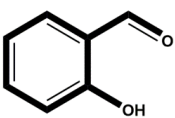
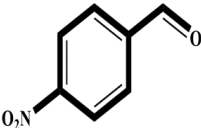
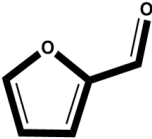


Figure 16 The influence of time for Aldol condensation reaction.

Reaction conditions: benzaldehyde (5 mmol), acetone (5 mmol), FeNPs/DETA@rGO (30 mg), solvent-free, temp. (50 °C), **time (X h)**.

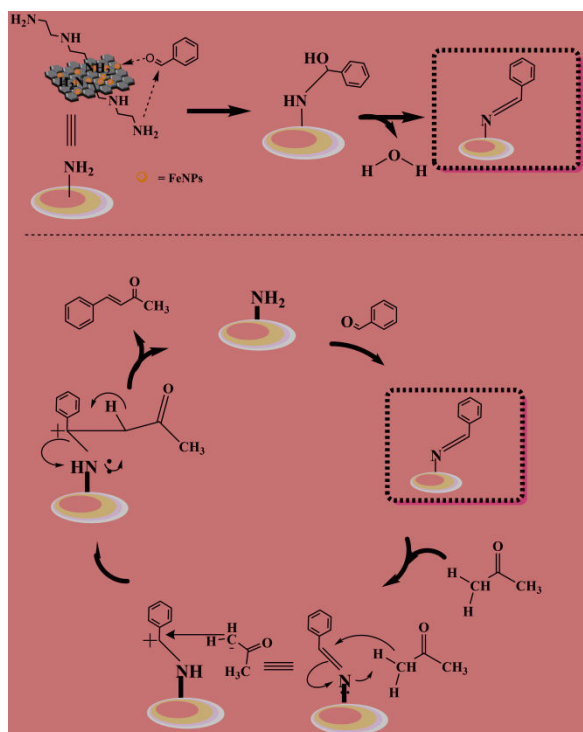
[6.8] Aldol condensation reaction using diverse aldehydes over FeNPs/DETA@rGO as a representative catalyst (Table 2)

$ \begin{array}{c} \text{R}-\text{CHO} \quad + \quad \text{CH}_3\text{COCH}_3 \xrightarrow[50^\circ\text{C}]{\text{FeNPs/DETA@rGO, 4 h}} \text{R}-\text{CH}=\text{CH}-\text{COCH}_3 \\ \text{(A)} \qquad \qquad \text{(B)} \qquad \qquad \qquad \qquad \qquad \qquad \qquad \qquad \text{(C)} \end{array} $			
Entry	Substrate (A)	Conversion (%)	Selectivity (%)
1		82.9	96.7
2		62.9	78.9
3		59.9	70.6
4		41.5	25.3
5		39.6	19.5
6		65.8	61.6

Reaction conditions: benzaldehyde (5 mmol), acetone (5 mmol), FeNPs/DETA@rGO (30 mg), solvent-free, temp. (50 °C), time (4 h).

After getting the optimized conditions, the next target was to extend and examined the reactions between diverse aldehyde derivatives and acetone for Aldol condensation reaction. As shown in Table 2, the reaction occurs between benzaldehyde and acetone over FeNPs/DETA@rGO as a representative catalyst and completed within 4 h, furnishing excellent conversion of benzaldehyde with benzylideneacetone product selectivity (Table 2, entry 1). Furthermore, acetone reacted prolifically with different benzaldehyde derivatives (such as 4-methyl benzaldehyde, 4-methoxy benzaldehyde, 2-hydroxy benzaldehyde, 4-nitro benzaldehyde and furfuraldehyde) under mild condition (i.e. Temp. 50 °C, Time 4 h, solvent-free) to achieve excellent conversion and selectivity (Table 2, entry 2-6). As far as the results are concerned (Table 2), the electron withdrawing groups have shown admirable conversion and selectivity except for 2-hydroxy benzaldehyde which has shown comparatively lower conversion and selectivity might be due to the steric hindrance aspect [43]. In addition, electron donating group i.e. 4-nitrobenzaldehyde with acetone exhibited comparable trend as of 2-hydroxy benzaldehyde [43]. Moreover, we have also tested heteroatom compound i.e. furfuraldehyde with acetone, altering to the desired results with tremendous conversion and product selectivity (Table 2).

[6.9] The plausible reaction mechanism for Aldol condensation reaction using FeNPs/DETA@rGO as a representative catalyst



Scheme 4 The plausible reaction mechanism for the Aldol condensation reaction using the FeNPs/DETA@rGO catalyst

The merely tentative reaction mechanism for the Aldol condensation reaction using FeNPs/DETA@rGO as a representative bifunctional catalyst (where FeNPs as Lewis acid and NH_2 groups of DETA as basic sites) is illustrated in Scheme 4. As shown in Scheme 4, the first step would involve the attachment of an aldehyde substrate to the FeNPs/DETA@rGO catalyst, forming a most basic aldimine intermediate. In the succeeding step, this aldimine intermediate can generate a carboanion ($\text{CH}_3\text{COCH}_2^-$) via in situ deprotonations of acetone molecule. In addition, FeNPs as Lewis acidic sites or FeNPs/DETA@rGO as a bifunctional catalyst can facilitate the addition reaction. The former one triggers the carbonyl group of an aldehydes, however; the latter act as a combination of Lewis acid-Brønsted base triggers and brings both reactants together, bestowing the desired product.

[6.10] Recyclability Test

For any heterogeneous catalytic system reusability of the catalyst is of vast importance. To examine the recyclability of FeNPs/DETA@rGO bifunctional catalyst for Henry and Aldol condensation reactions, the catalyst is first to separate from the reaction mixture by filtration, washed with distilled water several times followed by oven drying before employing for the further catalytic test. The results of each recycle tests are exemplified in Fig. 17. For the Henry reaction, the conversions in the fresh to fourth recycles are 92.7%, 92.7%, 92.7%, 92.7% and 91.6%. However, gradually dropped in the selectivity (i.e. 99.8% in fresh to 87.6% after 4th recyclability test) was observed [Fig. 17(A)]. The more or less similar trend was observed during the Aldol condensation reaction [Fig. 17(B)]. Indeed, due to the reciprocal action of metal-support interaction, FeNPs/DETA@rGO bifunctional catalyst is truly deserved as a heterogeneous catalyst.

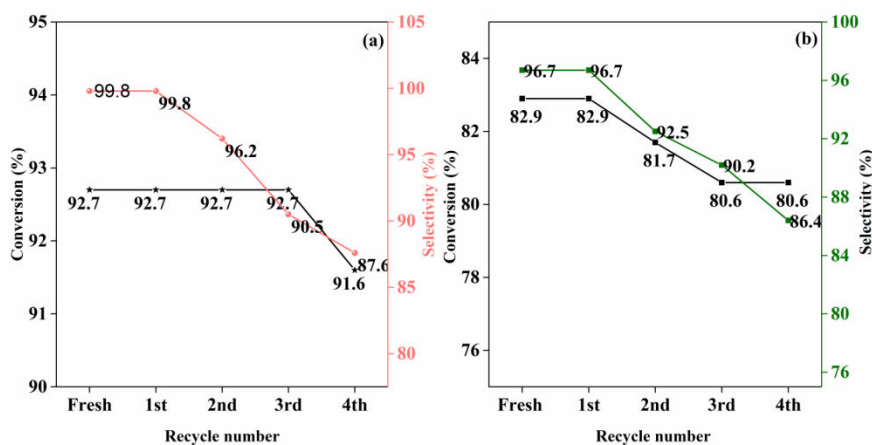


Figure 17 Recyclability tests of FeNPs/DEPT@rGO over (A) Henry reaction (B) Aldol condensation reaction.

(a) Henry reaction

Reaction conditions: benzaldehyde (5 mmol), nitromethane (5 mmol), FeNPs/DETA@rGO (20 mg), solvent-free, temp. (50 °C), time (3 h).

(b) Aldol condensation reaction

Reaction conditions: benzaldehyde (5 mmol), acetone (5 mmol), FeNPs/DETA@rGO (30 mg), solvent-free, temp. (50 °C), time (4 h).

[6.11] Conclusions

In recapitulate, we have exemplified that a pertinent design of FeNPs/DETA@rGO (a combination of FeNPs and amino groups from DETA) can be implanted onto the surface of reduced graphene oxide nanosheet to construct a bifunctional catalyst fascinating the features required for effectual catalysis. It possessed easily accessible active metal sites (with Lewis acid nature) and the basic sites generated through the modification of –COOH groups (present on GO) by amino groups of DETA. FeNPs/DETA@rGO has been efficiently used as a bifunctional catalyst for the β -nitrostyrene synthesis (with high yield up to 99.8%) for the Henry reaction of various substituted benzaldehydes with nitromethane under solvent-free condition. Furthermore, the aforesaid catalyst was also tested for Aldol condensation reaction using various substituted benzaldehydes with acetone under solvent-free condition offering high yield (96.7%) of benzylideneacetone product selectivity. This high efficacy could be attributed to the permutation effects of acid-base supportive actions as well as unique two-dimensional structure offered by reduced graphene oxide nanosheet. In addition, our study further demonstrates that it is truly heterogeneous in nature and recyclable up to four consecutive cycles without significant loss of activity.

[6.12] References

- [1] Y. Ono, *J. Catal.*, **216**, 406 (2003).
- [2] G. Busca, *Chem. Rev.*, **107**, 5366 (2007).
- [3] R. Dalpozzo, G. Bartoli, L. Sambri, P. Melchiorre, *Chem. Rev.*, **110**, 3501(2010).
- [4] F. Winter, V. Koot, A. J. van Dillen, J. W. Geus, K. P. de Jong, *J. Catal.*, **236**, 91 (2005).
- [5] A. Corma, H. Garcia, *Adv. Synth. Catal.*, **348**, 1391 (2006).
- [6] Edoardo Garrone, François Fajula, *Mol Sieves* **6**: 213 (2008).
- [7] J. A. Melero, R. van Grieken, G. Morales, *Chem. Rev.*, **106**, 3790 (2006).
- [8] D. E. De Vos, M. Dams, B. F. Sels, P. A. Jacobs, *Chem. Rev.*, **102**, 3615 (2002).
- [9] A. Corma, H. García, *Chem. Rev.*, **103**, 4307 (2003).

- [10] A. Dhakshinamoorthy, H. Garcia, *Chem. Soc. Rev.*, **41**, 5262 (2012).
- [11] A. Dhakshinamoorthy, M. Alvar, H. Garcia, *Chem. Commun.*, **48**, 11275 (2012).
- [12] Y. Ono, T. Baba, *Catal. Today*, **38**, 321 (1997).
- [13] J. J. Spivey, E. J. Doskocil, S. Bordawekar, R. J. Davis, in *Catalysis*, 72 (2000)
- [14] W. P. Jencks, *Acc. Chem. Res.*, **9**, 425 (1976).
- [15] H. P. Gong, W. M. Hua, Y. H. Yue, Z. Gao, *Appl. Surf. Sci.*, **397**, 44 (2017).
- [16] M. Oliverio, P. Costanzo, A. Macario, G. Luca, M. Nardi, A. Procopio, *Molecules* **19**(7), 10218 (2014).
- [17] A. K. Geim, K. S. Novoselov, *Nat. Mater.* **6** (3), 183 (2007).
- [18] C. K. Modi, R. Vithalani, D. Patel, An immense uprising: functionalization and fine-tuning of 2D graphene designed for heterogeneous catalysis to make things greener. In: A. K. Mishra, D. Pathania (eds) *Graphene oxide: advances in research and applications*. Nova Science Publishers, USA, 217 (2018).
- [19] R. Vithalani, D. Patel, C. K. Modi, N. N. Som, P. K. Jha, S.R. Kane, *Diam. Relat. Mater.* **90**, 154 (2018).
- [20] R. Vithalani, D. S. Patel, C. K. Modi, V. Sharma, P. K. Jha, *Appl. Organomet. Chem.* 5500, (2020)
- [21] Y. Wang, Z. Rong, Y. Wang, T. Wang, Q. Du, Y. Wang, J. Qu, *ACS Sustainable Chem. Eng.* **5**, 1538 (2017).
- [22] F. Zhang, H. Jiang, X. Wu, Z. Mao, H. Li, *ACS Appl. Mater. Interfaces*, **7**, 3, 1669 (2015).
- [23] S. Liu, L. Cheng, K. Li, C. Yin, H. Tang, Y. Wang, Z. Wu, *ACS Sustainable Chem. Eng.*, **7**, 8136 (2019).
- [24] D. Patel, R. Vithalani, C. K. Modi, *New J. Chem.*, **44**, 2868 (2020).
- [25] K. C. Nicolaou, P. G. Bulger, D. Sarlah, *Angew. Chem., Int. Ed.*, **44**, 4442 (2005).

- [26] G. Casiraghi, L. Battistini, C. Curti, G. Rassu, F. Zanardi, *Chem. Rev.*, **111**, 3076 (2011).
- [27] R. Kawahara, K.-i. Fujita, R. Yamaguchi, *J. Am. Chem. Soc.*, **134**, 3643 (2012)
- [28] R. Kawahara, K.-i. Fujita, R. Yamaguchi, *Angew. Chem., Int. Ed.*, **51**, 12790 (2012).
- [29] W. Zhang, H. Gu, Z. Li, Y. Zhu, Y. Li, G. Zhang, F. Zhang, X. Fan, J. *Mater. Chem. A*, **2**, 10239 (2014).
- [30] E. Rodrigo, B. G. Alcubilla, R. Sainz, J. L. Garcia Fierro, R. Ferritto, M. Belen Cid, *Chem. Commun.*, **50**, 6270 (2014).
- [31] R. Vithalani, D. Patel, C. K. Modi, N. N. Som, P. K. Jha, S.R. Kane, *Diam. Relat. Mater.* **90**, 154 (2018).
- [32] P. Mondal, A. Sinha, N. Salam, A. Roy, N. R. Jana, S. M. Islam, *RSC Adv*, **3**, 5615 (2013).
- [33] D. Patel, R. Vithalani, C. K. Modi, *New J. Chem.*, **44**, 2868 (2020).
- [34] M. M. Sk, C. Y. Yue, *RSC Adv.*, **4**, 19908 (2014).
- [35] D. Wang, Z. Li, *Catal. Sci. Technol.*, **5**, 1623 (2015).
- [36] A. C. Ferrari, *Solid State Commun.*, **143**, 47 (2007).
- [37] A. C. Ferrari, D. M. Basko, *Nat. Nanotechnol.*, **8**, 235 (2013).
- [38] J. B. Wu, X. Zhang, M. Ijas, W. P. Han, X. F. Qiao, X. L. Li, D. S. Jiang, A. C. Ferrari, P. H. Tan, *Nat. Commun.*, **5**, 5309 (1-8) (2014).
- [39] R. Bissessur, P.K.Y. Liu, S.F. Scully, *Synth. Met.* **156**, 1023 (2006).
- [40] B. Xue, J. Zhu, N. Liu, Y. Li, *Catal. Commun.*, **64**, 105 (2015).
- [41] L. C. R. Henry, *Acad. Sci. Ser. C*, **120**, 1265 (1895).
- [42] T. Nitabaru, A. Nojiri, M. Kobayashi, N. Kumagai, M. Shibasaki, *J. Am. Chem. Soc.*, **131**, 13860 (2009).
- [43] D. Wang, Z. Li, *Catal. Sci. Technol.*, **5**, 1623 (2015).
- [44] Y. Yang, H.-F. Yao, F.-G. Xi, E.-Q. Gao, *J. Mol. Catal. A Chem.*, **390**, 198 (2014).
- [45] J. B. M. de Resende Filho, G. P. Pires, J. M. G. de Oliveira Ferreira, E. E. S. Teotonio, J. A. Vale, *Catal. Letters*, **147**, 167 (2017).

